약학석사 학위논문

Evaluation of Epoxyketone-based Immunoproteasome-selective Inhibitors with Enhanced Brain Distribution and Stability *In Vitro* & *In Vivo*

뇌 조직으로의 분포 및 안정성이 개선된 epoxyketone-based 면역프로테아좀 억제제의 평가연구

2020 년 2 월

서울대학교 대학원

약학과 약제과학 전공

유 지 수

Abstract

Evaluation of Epoxyketone-based Immunoproteasome-selective Inhibitors with Enhanced Brain Distribution and Stability *In Vitro* & *In Vivo*

Jisu Yoo
Department of Pharmaceutical Sciences
The Graduate School
Seoul National University

Immunoproteasome (iP) is one of the proteasome subtypes and is induced by immune cytokines. Recent studies have reported that iP inhibitors are effective against neurodegenerative diseases. Among the iP inhibitors used in research, YU102 has an epoxyketone as a pharmacophore and has a peptides backbone. Proteasome inhibitors having epoxyketone and peptides are considered to have a short *in vivo* half-life. In addition, YU102 is known as the P-glycoprotein (P-gp) substrate, which is the main efflux transporter of the blood-brain barrier, thereby limiting the penetration to the brain. Therefore, in this study it is evaluated the

possibility of brain penetration *in vivo* for several YU102 derivatives. *In vivo* and *in vitro* stability was measured for macrocyclic YU102 analogs that are expected to increase metabolic stability. *In vitro* stability experiments using liver homogenate and whole blood in rats showed that the macrocyclic compounds (DB43, DB49) were generally more stable than the linear form (DB16). In particularly, DB43 showed a significant increase in stability in liver homogenate where metabolism occurs very rapidly. In addition, plasma concentrations were measured by mouse pharmacokinetic test. As a result, macrocyclic compounds (DB43, DB49) showed greater stability & systemic exposure than linear compounds (YU102, DB16). In addition, DB55 showed slightly increased *in vivo* stability compared to DB49. To determine the potential for penetration into the brain of the compounds, the degree of target (LMP2) inhibition in the brain was measured. Comparing between linear forms (YU102 vs DB16), the target brain was suppressed by about 20 % in the mouse brain injected with DB16. After injection of linear forms (YU102, DB16) or macrocyclic forms (DB43, DB49), the target inhibitions in the brain were reduced by about 8 % in DB43 or about 11 % in DB49 compared to vehicle group. In addition, the blood-to-plasma concentration ratios (B/P ratios) and plasma unbound fraction were measured in mice. As a result,

epoxyketone-based inhibitors showed a B/P ratio of greater than 1 and the unbound fractions of the rage of 54-77 % in all compounds except DB43. DB43 has a B/P ratio of about 1 and an unbound fraction of about 98 %, suggesting DB43 had a lower binding to erythrocyte. This study is to evaluate epoxyketone-based immunoproteasome-selective inhibitors with enhanced brain permeability & stability and demonstrated the potential of several compounds. While further research should be conducted, this study may suggest possibilities of epoxyketone-based immuno-proteasome inhibitors for brain distribution.

Keywords: immunoproteasome inhibitor, epoxyketone-based, brain distribution, macrocyclization

Student Number: 2018-26406

Contents

List of Tables

List of Figures

1. Introduction

Immunoproteasome (iP) is one of the subtypes of proteasome consisting of multi-catalytic subunits. Proteasome is a component of the ubiquitin-proteasome system that plays an essential role in cell survival by breaking down damaged or misfolded proteins[1]. The most abundant of several subtypes of proteasome is the constitutive proteasome (cP), and iP is derived from cP by stimulation of inflammatory cytokine such as interferon-gamma or tumor necrosis factor-alpha (TNF-α)[2,3]. iP is known to be present in certain cancers[4-8], autoimmune diseases[9-13], and neurodegenerative diseases[14] and plays an important in disease states. In particular, recent research suggested that iP inhibitors may be effective against neurodegenerative diseases, suggesting a novel class of drug for diseases with limited therapeutic options[15-17]. However, despite this potential, so far there is a lack of options for drugs with improved brain permeation.

Carfilzomib, the second generation of cP inhibitor approved by the US FDA in 2012, has epoxyketone as a pharmacophore and peptides as a backbone. Unlike bortezomib (first generation of cP inhibitor with US FDA approval in 2003, has bononic acid as a pharmacophore) that reversibly interact with the target,

epoxyketone-based cP inhibitors bind more selectively and irreversibly with the target[18]. YU102, a compound that selectively inhibits LMP2 (β1i) out of the iP catalytic subunits, exhibited selectivity and potency for LMP2 as an epoxyketone-based inhibitor[19]. However, in most cases, epoxyketone-based proteasome inhibitors are considered to have short *in vivo* half-lives that degrade rapidly *in vivo*. YU102 is also known as a substrate of P-glycoprotein (P-gp)[20], one of the main efflux transporters of the blood-brain barrier (BBB), which limits its penetration into the brain.

The YU102 analogs library was constructed by changing selected deformable parts through computational modeling. Among them, compounds used in this study were selected in consideration of selectivity & potency to LMP2 and P-gp interaction *in vitro*. YU102 derivatives can be divided into two classes: i) DB16 (Fig. 1A) is slightly modified and maintained the linear form of YU102, ii) DB43, DB49, and DB55 are macrocyclic forms. Macrocyclic compounds were thought to increase drug stability by having resistance to enzymes that degrade drugs with low accessibility due to steric hinderance, but the mechanism has not yet been fully identified[21-24]. The metabolic pathway study of Oprozomib, one of the epoxyketone-based proteasome inhibitors, suggested that a

large proportion of drugs were degraded by epoxide hydrolases (enzymes that degrades epoxyketone pharmacophores) and peptidases (enzymes that degrade peptides backbone)[25]. In addition, recent study has shown that orally available oprozomib-derived macrocyclic peptides were more metabolically stable and favorable inhibition against the target than oprozomib *in vivo*[26]. Therefore, it was assumed that macrocyclic compounds would increase stability by resisting theses enzymes.

Proteasome, which could bind to epoxyketone-based inhibitors (either low or high selectivity), was known to be very abundant in red blood cells (RBCs)[27] and these inhibitors were thought to exhibit high protein binding[28-30]. In the case of carfilzomib, the blood-to-plasma concentration (B/P) ratio was greater than 0.6[30] and the plasma unbound fraction was about 97%[31] in rats. Free drug concentration could influence for the drug to enter the target tissue according to the free drug hypothesis. Nevertheless, few studies about epoxyketone-based proteasome inhibitors have measured B/P ratios and protein binding (unbound fraction) in mice.

In this study, it is examined the *in vitro* & *in vivo* stability for YU102 analogs in rats and mice. Also, *in vivo* brain permeation was evaluated by measuring the degree of inhibition of LMP2, a

target of compounds in the mouse brain. Finally, B/P ratio and plasma protein binding were measured in mice. Taken together, by assessing the above, the brain distribution potential of epoxyketone-based immunoproteasome inhibitors can be evaluated.

2. Materials and methods

2.1. YU102 derivative compounds

YU102 (MW: 514.61), DB16 (MW: 578.67), DB43 (MW: 555.716), DB49 (MW: 451.564), and DB55 (MW: 469.5544) were provided by Dr. Kyung Bo Kim (Department of Pharmaceutical Sciences, University of Kentucky, Lexington KY 40536-0596, USA).

2.2. *In vitro* metabolic stability in SD rat liver homogenates and whole blood

To investigate whether the macrocyclic compounds show improved metabolic stability over linear forms, the rate by which compounds disappear in the rat liver homogenates or whole blood was measured. Sprague-Dawley rats (SD rats, seven-week-old, male) were purchased from CLS Bio (Bucheon, Korea) and the protocol approved by the Seoul National University (SNU) Institutional Animal Care and Use Committee (approval No. 181019-7). The liver was harvested, washed and homogenized using Ultra Turrax homogenizer (IKA, Staufen, Germany) with five-fold excess volume of ice-cold phosphate-buffered saline (PBS, pH 7.4) per gram of tissue. The whole blood was collected by

heart puncture and heparinized at the final concentration of 25 IU/mL. The liver homogenate and whole blood were pre-incubated at 37℃ for 10 min and incubated with compounds at the final concentration of 1 μM (compounds dissolved in dimethyl sulfoxide, N=4). After short vortexing, an aliquot (40 uL) of the reaction mixture was taken and quenched with 160 μL of ice-cold acetonitrile (ACN) containing chlorpropamide (an internal standard, IS, 2.5 μg/mL) at pre-determined time points (0, 5, 10, 20, or 40 min). The mixture was vortexed for 10 min, centrifuged at 13,000 rpm for 10 min at 4℃. The drug levels in the resulting supernatant were quantified via HPLC interfaced with mass spectrometry system (LC-MS/MS, Agilent 6460 Triple Quad LC-MS system, Agilent Technologies, Palo Alto, CA).

The chromatographic separation was performed using a Phenomenex Luna C18 column (50 X 2.0 mm id, 3 μm, Agilent Technologies, Palo Alto, CA) and an isocratic mobile phase composed of acetonitrile:water (15:85, v/v) containing 0.1% formic acid at a flow rate of 0.3 mL/min. In a positive electrospray ionization mode, gas temperature, the fragment voltage, collision energy, and cell accelerator voltage were set as follows: 325 ℃, 150 V, 20 V, and 4 V for YU102; 325 ℃, 150 V, 45 V, and 4 V for DB16; 325 ℃, 114 V, 28 V, and 4 V for DB43; 325 ℃, 84 V, 44 V,

and 4 V for DB49; 325 ℃, 124 V, 30 V, and 5 V for DB55. Quantification was performed in the multiple reaction monitoring (MRM) mode using the following transitions: *m/z* 515.3 to 197.1 for YU102; *m/z* 579.3 to 70.25 for DB16; *m/z* 556.3 to 329.3 for DB43; *m/z* 452.3 to 70.1 for DB49; 470.3 to 88.1 for DB55. Chlorpropamide (an internal standard) were detected in the positive electrospray ionization mode (m/z 277.05 to 174.95).

2.3. Plasma pharmacokinetic (PK) study in ICR mice

ICR mice (7-week-old, male) were obtained from CLS Bio (Bucheon, Korea) and were acclimatized at the animal research facility in SNU. All animal experiments were conducted in accordance with the protocols approved by the Institutional Animal Care and Use Committee of SNU (SNU-181019-7-1). Compounds were injected via tail vein and blood samples (15-20 μL) were collected at the pre-determined time points (2, 15, 30, 60, 120 min from the retro-orbital plexus of the mice using microhematocrit tubes and 240 min from cardiac puncture using heparinized syringe). Collected blood samples were centrifuged at 13,000 rpm for 10 min at 4℃ and the resulting plasma samples was snap-frozen until analysis. To assess the compound levels in plasma, samples were processed for liquid-liquid extraction by mixing with tertiary butyl

methyl ether (tBME) containing carfilzomib (IS, 100 nM). After vortex for 10 min and centrifugation (13,000 rpm for 10 min at 4℃), the supernatant was evaporated overnight and reconstituted with ACN to analyze via LC-MS/MS (Conditions are described above). Chlorpropamide (an internal standard) were detected in the positive electrospray ionization mode (m/z 277.05 to 175.10). PK parameters were calculated by non-compartmental method.

2.4. LMP2 activity measurement in tissue homogenates from drug treated mice

Compounds were injected via intraperitoneal administration at the dose of 10 mg/kg (Fig. 4A) or tail vein injection at the dose of 5 mg/kg or 10 mg/kg (Fig. 4B) into ICR mice (7-week-old, male, n=4-8 per group). Blood samples were collected via cardiac puncture with a heparinized syringe and tissues were harvested 4 h after injection, weighed, and frozen at -80℃.

The tissue samples were homogenized adding the PBS (0.2 g tissue per mL PBS). The homogenized tissues were mixed with the same volume of passive lysis buffer (Promega, Madison, WI, USA). The supernatant was collected after vortex for 10 min and centrifugation (13,000 rpm) for 10 min at 4℃ and used for LMP2 activity assay (50 or 150 μg total protein/well for tissues, 0.2 μ

L/well for the whole blood and verified to be within the linear rage of the assay). The fluorogenic probe substrate Ac-Pro-Ala-Leu-7-amino-4-methylcoumarin (Ac-PAL-AMC, Boston Biochem, USA) were used to measure the levels of LMP2-specific catalytic activity at the final concentration of 100 μM in the assay buffer (20 mM Tris-Cl buffer (pH 8.0) and 500 μM EDTA). Free AMC was released and generate fluorescence signals. The initial cleavage signals were monitored every minute for 1 h via a SpectraMax M5 microplate multi-reader device (Molecular Devices) using excitation, emission and cut-off wavelengths of 360, 460 and 420 nm, respectively. The slopes were used as the initial hydrolysis rates for individual wells, calculated via linear regression and %normalized to the slope values from vehicle-treated control wells. Regression analysis was performed using GraphPad Prism 8.2.0.

2.5. Blood-to-Plasma concentration (B/P) ratio and Plasma protein binding assessment

Compounds were added to fresh pre-warmed blank blood of mice at final concentration of 0.2, 2, 10 μM, and the mixture was incubated at 37℃ for 15 min. After incubation, the mixture was centrifuged (13,000 rpm) and the plasma was collected as the

supernatant (A). Also, compounds were added to blank plasma at the final concentration of 0.2, 2, 10 uM (B). Compounds were extracted by protein precipitation method using acetonitrile with an IS (Chlorpropamide). The response of compounds was then determined by LC-MS/MS analysis to calculate the blood-to-plasma concentration ratios. B/P ratios were calculated by response (analytic peak area to an IS) of (B) divided by response of (A).

The extent of plasma protein binding was also determined by the rapid equilibrium dialysis method, according to the manufacturer's recommended protocol (Thermo Fisher Scientific, Waltham, MA). Briefly, the dialysis plate was rinsed with 20% ethanol 3 times for 10 min and washed with filtered water 2 times for 10 min. 1 μM as a final concentration was added to the mouse plasma (donor chamber, 200 μL/well) and protein-free phosphate buffer (PBS, pH adjusted to 7.4) was added to the receiver chamber (400 μL/well) (n=3-4, independent chambers). The plate was sealed and incubated on a shaker (300 rpm) at 37℃ for 2 hours. After the incubation, a 50 μL of aliquot was collected from each side of the chamber. To ensure that the matrix of the samples matched, a 50 μL aliquot of blank medium was then added to the PBS sample, and a one volume of PBS was also added to the plasma sample. The resulting sample was then analyzed via LC-MS/MS to

determine the unbound fraction (f_u).

2.6. Statistical analysis

All results are presented as mean ± standard deviation (SD) of the replicates. To determine statistical significance, Student's *t*-test with a Tukey's *post-hoc* test or ANOVA followed by Dunnett's *post-hoc* test was performed using GraphPad Prism (GraphPad Software, version 8.2.0). A p-value < 0.05 was considered statistically significant.

3. Results

3.1. *In vitro* metabolic stability comparison in SD rats

In the rat liver homogenates, the macrocyclic compound DB43 showed improved stability markedly compared to other compounds (especially, linear compounds YU102 and DB16) (Fig. 2A). The remaining compounds at 10 min were 41.0 ± 7.1, 12.1 ± 3.1, 13.9 ± 7.1, 2.9 ± 0.4 % for DB43, DB49, YU102 and DB16, respectively. In whole blood, the rate of drug degradation during the same time is slower than that of liver homogenate. Comparing the %remaining drug values at the 40min were 58.4 ± 0.6, 84.4 ± 6.0, 70.6 ± 4.0, 42.4 ± 7.2 % for DB49, DB43, YU102 and DB16, respectively (Fig 2B). Unlike the liver homogenate results, where DB43 showed the greatest stability, DB49 showed the best stability at 20 min and 40 min.

3.2. *In vivo* plasma pharmacokinetics in ICR mice

To determine the stability of compounds *in vivo*, pharmacokinetic profiles were compared. ICR mice received 5 or 10 mg/kg of compound via tail vein injection. The plasma concentrations of linear forms (YU102 and DB16) decreased rapidly. In comparison, at all the time points except 240 min, the

remaining plasma concentrations of the macrocyclic compounds (DB43, DB49) were higher than those of linear forms (Fig 3A). In addition, macrocyclic compounds administered at 5 mg/kg dose showed greater systemic exposure compared to linear forms: the plasma area-under-the curve from time 0 to infinity (AUC_{inf}) were 129.0, 50.5, 39.9, and 14.9 μg · min/mL for DB43, DB49, YU102, and DB16, respectively (Table 1). AUC up to the last time point was verified as more than 97% of AUC_{inf}. Consequently, DB43 and DB49 showed lower clearance values and smaller volume of distribution at steady state (V_{ss}) than YU102 and DB16 (CL, 42.3, 101.6, 129.4, and 363.6 mL/min/kg; V_{ss}, 1178.7, 571.2, 1988.3, and 1303.8 mL/kg for DB43, DB49, YU102, and DB16, respectively). These results indicate that macrocyclic compounds (DB43, DB49) showed enhanced *in vivo* stability, rendering a promising potential to enter the brain. Also, comparing the PK parameters with DB49 and DB55 when 10 mg/kg dose is administered to the mice, DB55 showed slightly higher systemic exposure (AUC_{inf}) than DB49 (72.4 μg · min/mL for DB49 and 85.2 μg · min/mL or DB55).

3.3. *In vivo* LMP2 immunoproteasomal inhibition in the brain and other tissues

To determine the potential for brain penetration for LMP2

inhibitor candidates known to have less P-gp interaction and improved *in vitro* & *in vivo* metabolic stability, the extent of %remaining LMP2 activity in the brain at 4 h after single dose injection was measured. When the remaining LMP2 activity of DB16 (known to have less interaction with P-gp) and YU102 (known to as P-gp substrate) was assessed, the results indicated that the systemically administered YU102 and DB16 effectively inhibited the LMP2 activity in major organs (i.e. whole blood, liver, spleen and lung) (Fig. 4A). With the same dose of 10 mg/kg was administration (i.p.), YU102 was more effective in inhibiting the LMP2 activity than DB16 in these tissues. In contrast, YU102 did not inhibit the LMP2 activity in the brain. In case of DB16, there was a decreasing trend in the LMP2 activity at 4 h post-dosing (approximately 20% inhibition, p value 0.07 when compared DB16 with vehicle group in the brain).

Single i.v. injection at the dose of 5 mg/kg was conducted to compare the brain penetration of macrocyclic compounds (DB43 and DB49) and linear forms (YU102 and DB16), and remaining LMP2 activity after 4 h injection in the brain and whole blood was measured (Fig. 4B). Consistent with the above results (Fig. 4A), YU102 strongly inhibited LMP2 in whole blood compared to DB16. In addition, the result of the inhibition potency in whole blood

showed DB49, YU102, DB16, and DB43 were larger in order (% inhibition 89.37 ± 0.63, 77.41 ± 4.47, 61.01 ±10.65, and 52.19 ± 9.33, respectively). However, when comparing inhibition in the brain which is protected by intact BBB, DB43 and DB49 showed approximately 8 and 11% inhibition (p value is 0.3330 and 0.0451, respectively, when compared with vehicle group).

3.4. Blood-to-Plasma concentration (B/P) ratios and Plasma protein binding in mice

The B/P ratios at concentrations of 0.2, 2, and 10 μM assessed as follows: 1.96, 1.92, and 1.73 for YU102; 13.87, 9.66, and 6.88 for DB16; 0.81, 0.71, and 1.04 for DB43; 1.35, 1.32, and 1.50 for DB49; 1.56, 1.62, and 1.77 for DB55, respectively. The B/P ratio of carfilzomib was measured as a positive control and the values were 0.71, 0.75, and 0.60 at concentrations of 0.2, 2, and 10 μM which were comparable to reported values (0.82, 0.74, and 0.63 in the rat[30], respectively).

The representative (i.e., averaged) unbound fraction in the mouse plasma ($f_{u,plasma}$) values of compounds were calculated as follows: 65.18 ± 5.88 for YU102; 73.05 ± 5.64 for DB16; 98.36 ± 0.34 for DB43; 76.58 ± 0.84 for DB49; 72.12 ± 2.90 for DB55, respectively (n=6-7). As a positive control, $f_{u,plasma}$ of carfilzomib

was measured. The resulting value was 98.31% ± 1.52 and it is comparable to reported value (97.6−98.2% in human blood[31]).

4. Discussion

Because of the robustness of the blood-brain barrier, the development of CNS penetrable drugs has been considered a challenging task. However, with the aging of the population, the number of patients suffering from neurodegenerative diseases is steadily increasing (neurodiscovery.harvard.edu), and the necessity of developing brain penetrable drugs is growing. In addition, despite the excellent effects of the epoxyketone-based proteasome inhibitors, various formulations have been tried to overcome the short *in vivo* half-life. In this study, it is evaluated that the YU102 modified compounds could be potential in brain distribution by testing stability and target inhibition in brain.

As we hypothesized, macrocyclic compounds tend to have improved *in vitro* & *in vivo* stability compared to linear forms (Fig. 2, Fig. 3). In particular, the increased stability of DB43 in rat homogenate (Fig. 2A), in which drug metabolism progresses rapidly, is thought to have a greater effect on the stability in the *in vivo* PK test (Fig. 3). However, not all macrocyclic compounds showed improved stability over linear forms in some time points. *In vitro* stability test using liver homogenate and whole blood in rats showed that YU102 had a greater %drug residual than DB49 and DB43,

respectively (Fig. 2). That is, in addition to inhibition of metabolism of compounds by cyclization, other mechanisms affecting *in vivo* stability were thought to exist.

Experiments examining the extent of *in vivo* target inhibition suggest that the mechanism of avoiding P-gp interaction played an important role in BBB permeation (Fig. 4A). These results suggest that YU102 which was more stable than DB16 can potently inhibit LMP2 which is readily accessible, but not LMP2 present in the brain behind the functional intact BBB. These results are in line with YU102 being a substrate for P-gp. Therefore, these results indicated that DB16 could achieve CNS penetration and engage LMP2 target interactions in the brain parenchyma, possibly an improved efficacy over YU102. In addition, the results of experiments in which different injection method and dose (i.v. injection and 5 mg/kg) were injected into mice showed that macrocyclic compounds (DB43, DB49) with better stability slightly reduced LMP2 in brain compared to linear forms (YU102, DB16). These results indicated that stability improvement may also have a positive effect on the drug's target inhibition in the brain (efficacy).

Recently, dual inhibition of LMP2 (β1i) and LMP7 (β5i) has been shown to suppress Alzheimer's disease[37] or tumor

growth progression[8]. Since the development of proteasome inhibitors, many research have focused on the major catalytic subunits $\beta5/\beta5i$. However, as research on other catalytic subunits progresses, inhibition of other subunits has also been shown to be effective against some diseases, and studies have shown that dual inhibition has a greater effect[11,37,38]. Thus, LMP2 inhibitors used in this study may also be more potent by co-administration with inhibitors that selectively interact with other subunits.

The B/P ratios of all the compounds except DB43 are greater than 1 and showed lower plasma unbound fraction than carfilzomib. B/P ratios greater than 1 were usually the result of the distribution of the drug in red blood cells and the low unbound fraction meant greater binding with proteins in the body. However, DB43 showed the lowest B/P ratio and the highest $f_{u,plasma}$. Therefore, it can be predicted that DB43 might be the most limited distribution to non-target tissue (V_{SS} ~571.2 ml/kg) and it is possible that it may influenced for enhanced brain distribution. The linear and macrocyclic structures did not seem to differ in B/P ratio and protein binding.

In conclusion, our results could support that the possibility of penetrating into the brain of YU102 analogs. Some recent studies indicated a promising therapeutic potential of YU102 in Alzheimer'

s disease models[17]. By improving the CNS penetration using epoxyketone-based immunoproteasome-selective inhibitors, we may achieve the target engagement (LMP2 inhibition) in the brain more effectively (using lower doses) and possible therapeutic effects with minimal side effects, though it remains to be verified whether or not these compounds show efficacy in diseased animal models.

5. References

1. Livneh I, Cohen-Kaplan V, Cohen-Rosenzweig C, Avni N, Ciechanover A 2016. The life cycle of the 26S proteasome: from birth, through regulation and function, and onto its death. Cell Res 26(8):869-885.
2. Aki M, Shimbara N, Takashina M, Akiyama K, Kagawa S, Tamura T, Tanahashi N, Yoshimura T, Tanaka K, Ichihara A 1994. Interferon-gamma induces different subunit organizations and functional diversity of proteasomes. Journal of biochemistry 115(2):257-269.
3. Kimura H, Caturegli P, Takahashi M, Suzuki K 2015. New Insights into the Function of the Immunoproteasome in Immune and Nonimmune Cells. Journal of immunology research 2015:541984.
4. Rouette A, Trofimov A, Haberl D, Boucher G, Lavallee VP, D'Angelo G, Hebert J, Sauvageau G, Lemieux S, Perreault C 2016. Expression of immunoproteasome genes is regulated by cell-intrinsic and -extrinsic factors in human cancers. Scientific reports 6:34019.
5. Cloos J, Roeten MS, Franke NE, van Meerloo J, Zweegman S, Kaspers GJ, Jansen G 2017. (Immuno)proteasomes as therapeutic target in acute leukemia. Cancer metastasis reviews 36(4):599-615.
6. Kuhn DJ, Hunsucker SA, Chen Q, Voorhees PM, Orlowski M, Orlowski RZ 2009. Targeted inhibition of the immunoproteasome is a potent strategy against models of multiple myeloma that overcomes resistance to conventional drugs and nonspecific proteasome inhibitor

s. Blood 113(19):4667-4676.

7. Singh AV, Bandi M, Aujay MA, Kirk CJ, Hark DE, Raje N, Chauhan D, Anderson KC 2011. PR-924, a selective inhibitor of the immunoproteasome subunit LMP-7, blocks multiple myeloma cell growth both in vitro and in vivo. British journal of haematology 152(2):155-163.
8. Wehenkel M, Ban JO, Ho YK, Carmony KC, Hong JT, Kim KB 2012. A selective inhibitor of the immunoproteasome subunit LMP2 induces apoptosis in PC-3 cells and suppresses tumour growth in nude mice. British journal of cancer 107(1):53-62.
9. Basler M, Mundt S, Bitzer A, Schmidt C, Groettrup M 2015. The immunoproteasome: a novel drug target for autoimmune diseases. Clinical and experimental rheumatology 33(4 Suppl 92):S74-79.
10. Basler M, Dajee M, Moll C, Groettrup M, Kirk CJ 2010. Prevention of experimental colitis by a selective inhibitor of the immunoproteasome. Journal of immunology (Baltimore, Md : 1950) 185(1):634-641.
11. Basler M, Lindstrom MM, LaStant JJ, Bradshaw JM, Owens TD, Schmidt C, Maurits E, Tsu C, Overkleeft HS, Kirk CJ, Langrish CL, Groettrup M 2018. Co-inhibition of immunoproteasome subunits LMP2 and LMP7 is required to block autoimmunity. EMBO reports 19(12).
12. Muchamuel T, Basler M, Aujay MA, Suzuki E, Kalim KW, Lauer C, Sylvain C, Ring ER, Shields J, Jiang J, Shwonek P, Parlati F, Demo

SD, Bennett MK, Kirk CJ, Groettrup M 2009. A selective inhibitor of the immunoproteasome subunit LMP7 blocks cytokine production and attenuates progression of experimental arthritis. Nature medicine 15(7):781-787.

13. Verbrugge SE, Scheper RJ, Lems WF, de Gruijl TD, Jansen G 2015. Proteasome inhibitors as experimental therapeutics of autoimmune diseases. Arthritis research & therapy 17:17.
14. Johnston-Carey HK, Pomatto LC, Davies KJ 2015. The Immunoproteasome in oxidative stress, aging, and disease. Critical reviews in biochemistry and molecular biology 51(4):268-281.
15. Bentea E, Verbruggen L, Massie A 2017. The Proteasome Inhibition Model of Parkinson's Disease. J Parkinsons Dis 7(1):31-63.
16. Bonet-Costa V, Pomatto LC, Davies KJ 2016. The Proteasome and Oxidative Stress in Alzheimer's Disease. Antioxid Redox Signal 25(16):886-901.
17. Yeo IJ, Lee MJ, Baek A, Miller Z, Bhattarai D, Baek YM, Jeong HJ, Kim YK, Kim D-E, Hong JT, Kim KB 2019. A SELECTIVE INHIBITOR OF THE IMMUNOPROTEASOME ATTENUATES DISEASE PROGRESSION IN MOUSE MODELS OF ALZHEIMER' S DISEASE. Alzheimer's & Dementia 15(7, Supplement):P1592.
18. Redic K 2013. Carfilzomib: a novel agent for multiple myeloma. The Journal of pharmacy and pharmacology 65(8):1095-1106.
19. Kreidenweiss A, Kremsner PG, Mordmuller B 2008. Comprehensive study of proteasome inhibitors against Plasmodium falciparum labo

ratory strains and field isolates from Gabon. Malaria journal 7:187.

20. Bhattarai D, Lee M, Baek A, Yoo Z, Miller Z, Baek Y, Yeo I, Hong J, Lee S, Lee W, Kim D-E, Kim K 2019. CNS-penetrant LMP2 Inhibitors as Potential Therapies for Age-related Macular Degeneration. SSRN Electronic Journal.
21. Chua KC, Pietsch M, Zhang X, Hautmann S, Chan HY, Bruning JB, Gutschow M, Abell AD 2014. Macrocyclic protease inhibitors with reduced peptide character. Angew Chem Int Ed Engl 53(30):7828-7831.
22. Driggers EM, Hale SP, Lee J, Terrett NK 2008. The exploration of macrocycles for drug discovery--an underexploited structural class. Nature reviews Drug discovery 7(7):608-624.
23. Marsault E, Peterson ML 2011. Macrocycles are great cycles: applications, opportunities, and challenges of synthetic macrocycles in drug discovery. Journal of medicinal chemistry 54(7):1961-2004.
24. Morrison C 2018. Constrained peptides' time to shine? Nature reviews Drug discovery 17(8):531-533.
25. Wang Z, Fang Y, Teague J, Wong H, Morisseau C, Hammock BD, Rock DA, Wang Z 2017. In Vitro Metabolism of Oprozomib, an Oral Proteasome Inhibitor: Role of Epoxide Hydrolases and Cytochrome P450s. Drug metabolism and disposition: the biological fate of chemicals 45(7):712-720.
26. Li D, Zhang X, Ma X, Xu L, Yu J, Gao L, Hu X, Zhang J, Dong X, Li J, Liu T, Zhou Y, Hu Y 2018. Development of Macrocyclic Pepti

des Containing Epoxyketone with Oral Availability as Proteasome Inhibitors. Journal of medicinal chemistry.

27. Davies KJ, Goldberg AL 1987. Proteins damaged by oxygen radicals are rapidly degraded in extracts of red blood cells. The Journal of biological chemistry 262(17):8227-8234.

28. Gupta N, Hanley MJ, Venkatakrishnan K, Perez R, Norris RE, Nemunaitis J, Yang H, Qian MG, Falchook G, Labotka R, Fu S 2016. Pharmacokinetics of ixazomib, an oral proteasome inhibitor, in solid tumour patients with moderate or severe hepatic impairment. Br J Clin Pharmacol 82(3):728-738.

29. Perel G, Bliss J, Thomas CM 2016. Carfilzomib (Kyprolis): A Novel Proteasome Inhibitor for Relapsed And/or Refractory Multiple Myeloma. P T 41(5):303-307.

30. Yang J, Wang Z, Fang Y, Jiang J, Zhao F, Wong H, Bennett MK, Molineaux CJ, Kirk CJ 2011. Pharmacokinetics, Pharmacodynamics, Metabolism, Distribution and Excretion of Carfilzomib in Rats. Drug Metabolism and Disposition:dmd.111.039164.

31. Wang Z, Yang J, Kirk C, Fang Y, Alsina M, Badros A, Papadopoulos K, Wong A, Woo T, Bomba D, Li J, Infante JR 2013. Clinical pharmacokinetics, metabolism, and drug-drug interaction of carfilzomib. Drug metabolism and disposition: the biological fate of chemicals 41(1):230-237.

32. Bohnert T, Gan L-S 2013. Plasma protein binding: From discovery to development. Journal of pharmaceutical sciences 102(9):2953-

2994.

33. Yim D-S 2019. Potency and plasma protein binding of drugs in vitro-a potentially misleading pair for predicting in vivo efficacious concentrations in humans. Korean J Physiol Pharmacol 23(4):231-236.

34. Park JE, Chun SE, Reichel D, Min JS, Lee SC, Han S, Ryoo G, Oh Y, Park SH, Ryu HM, Kim KB, Lee HY, Bae SK, Bae Y, Lee W 2017. Polymer micelle formulation for the proteasome inhibitor drug carfilzomib: Anticancer efficacy and pharmacokinetic studies in mice. PLoS One 12(3):e0173247.

35. Park JE, Park J, Jun Y, Oh Y, Ryoo G, Jeong YS, Gadalla HH, Min JS, Jo JH, Song MG, Kang KW, Bae SK, Yeo Y, Lee W 2019. Expanding therapeutic utility of carfilzomib for breast cancer therapy by novel albumin-coated nanocrystal formulation. Journal of controlled release : official journal of the Controlled Release Society 302:148-159.

36. Noda C, Tanahashi N, Shimbara N, Hendil KB, Tanaka K 2000. Tissue distribution of constitutive proteasomes, immunoproteasomes, and PA28 in rats. Biochemical and biophysical research communications 277(2):348-354.

37. Yeo IJ, Lee MJ, Baek A, Miller Z, Bhattarai D, Baek YM, Jeong HJ, Kim YK, Kim DE, Hong JT, Kim KB 2019. A dual inhibitor of the proteasome catalytic subunits LMP2 and Y attenuates disease progression in mouse models of Alzheimer's disease. Scientific reports

9(1):18393.

38. Johnson HWB, Lowe E, Anderl JL, Fan A, Muchamuel T, Bowers S, Moebius D, Kirk C, McMinn DL 2018. A required immunoproteasome subunit inhibition profile for anti-inflammatory efficacy and clinical candidate KZR-616 ((2S,3R)-N-((S)-3-(cyclopent-1-en-1-yl)-1-((R)-2-methyloxiran-2-yl)-1-oxopropan-2 -yl)-3-hydroxy-3-(4-methoxyphenyl)-2-((S)-2-(2-morpholinoacetamido)propanamido)pr openamide). Journal of medicinal chemistry.

Table 1. Pharmacokinetic (PK) parameters following the single in travenous administration of YU102, DB16, DB43, DB49, and DB55 to ICR mice

PK parameter (unit)	YU102	DB16	DB43	DB49		DB55
Dose (mg/kg)	5	5	5	5	10	10
AUC_{inf} (μg•min/mL)	39.9 ± 7.2	14.9 ± 4.5	129.0 ± 37.4	50.5 ± 9.8	72.4 ± 13.3	85.2 ± 10.0
MRT (min)	16.4 ± 12.7	3.5 ± 1.4	28.0 ± 11.9	5.7 ± 2.9	7.0 ± 4.9	5.0 ± 0.8
CL (mL/min/kg)	129.4 ± 28.4	363.6 ± 119.6	42.3 ± 15.6	101.6 ± 16.1	142.7 ± 27.7	118.6 ± 13.6
V_{SS} (mL/kg)	1988.3 ± 1377.0	1303.8 ± 717.8	1178.7 ± 644.6	571.2 ± 326.8	1091.5 ± 970.3	600.6 ± 143.0

AUC_{inf}, area under the concentration−time curve from time 0 to infinity; MRT, Mean residence time; CL, clearance; V_{ss}, volume of distribution at steady state. Mean values and S.D. from different individuals.

Table 2. Blood-to-Plasma concentration (B/P) ratio and Plasma unbound fraction ($f_{u,plasma}$) of YU102, DB16, DB43, DB49, and DB 55

Parameter		YU102	DB16	DB43	DB49	DB55
Blood-to-Plasma concentration ratio*	0.2 μM	1.96	13.87	0.81	1.35	1.56
	2 μM	1.92	9.66	0.71	1.32	1.62
	10 μM	1.73	6.88	1.04	1.50	1.77
$f_{u,plasma}$**		65.18 ± 5.88	73.05 ± 5.64	98.36 ± 0.34	76.58 ± 0.84	72.12 ± 2.90

* values are mean of two independent experiments (triplicate runs for each experiment)

** Data are expressed as means ± S.D. (n=6-7 independent batches)

Figure 1. Structures of epoxyketone-based LMP2 inhibitors, YU102 and YU102 analogs.

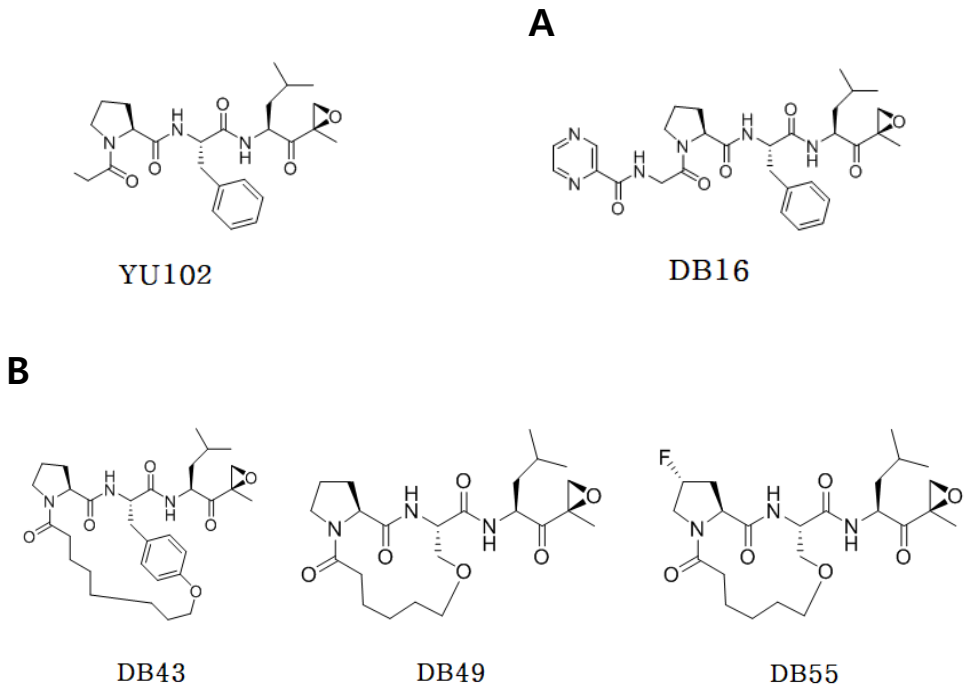

(A) Linear form, DB16. (B) Macrocyclic forms, DB43, DB49, and DB55.

Figure 2. *In vitro* stability of YU102, DB16, DB43, DB49, and carfilzomib.

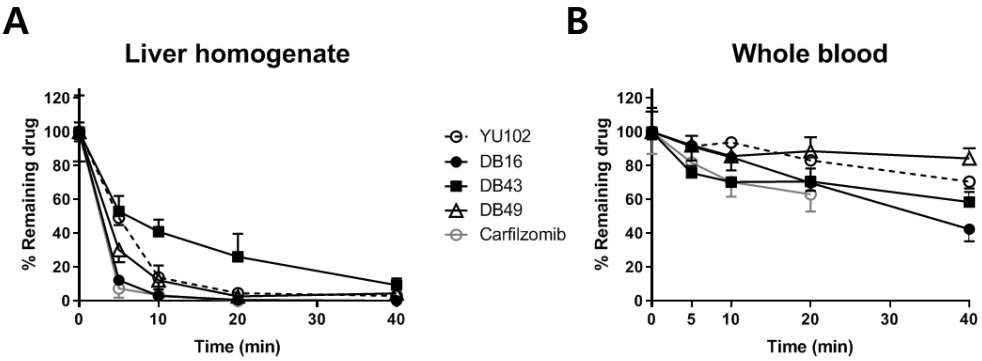

The level of remaining compounds was measured in rat liver homogenate (A) and whole blood (B). Compounds were incubated at a concentration of 1 μM at 0 min. Data are expressed as means ± S.D. of quadruplicates.

Figure 3. Temporal profiles for the plasma concentration of YU102, DB16, DB43, DB49, and DB55

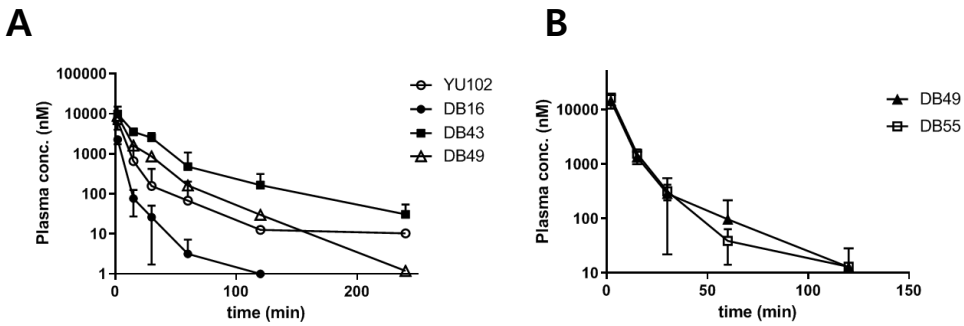

Plasma pharmacokinetic profiles after the intravenous administration of compounds at the dose of 5 mg/kg (A) or 10 mg/kg (B) in ICR mice. Mean ± S.D.

Figure 4. Inhibition of the LMP2 activity of YU102, DB16, DB43, and DB49 in the brain and major tissues.

A

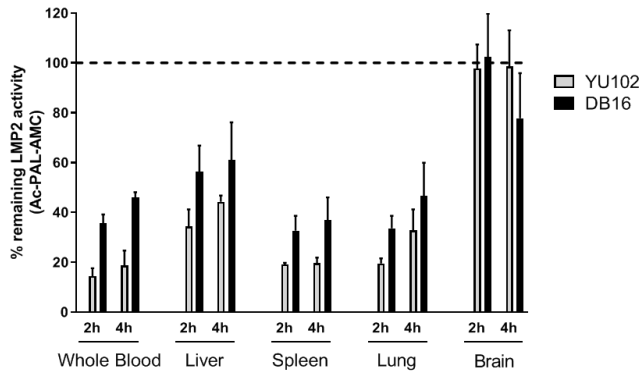

B

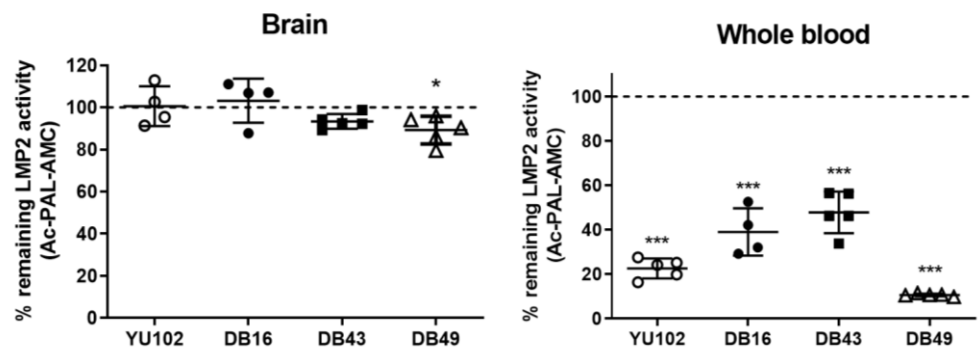

Y-axis represent the % remaining LMP2 activity 2 h or 4 h after the intraperitoneal injection of 10 mg/kg YU102 or DB16 (A) or 4 h after the intravenous bolus administration of 5 mg/kg YU102, DB16, DB43, and DB49 (B) (n=4-5). The tissue supernatant (50 μg organ, (A); 200 μg organ, (B)) or blood mixture (2 μL) was incubated in each well.

국문초록

면역프로테아좀 (Immunoproteasome, iP)은 프로테아좀 subtypes 중 하나로 면역 사이토카인에 의해 유도된다. iP는 특정 질병 상태에서 발현되는 것으로 알려져 있으며, 최근 연구에서는 iP 억제제가 신경퇴행성 질병에 대해 효과를 나타낸다고 보고되었다. 연구용으로 사용되는 iP 억제제 중 YU102는 epoxyketone을 pharmacophore와 peptides 골격을 가진다. 이 같은 공통구조를 가지는 억제제의 경우 짧은 *in vivo* 반감기를 가지는 것으로 생각된다. 또한, YU102의 경우 혈관-뇌 장벽 (blood-brain barrier)의 주요 efflux transporter인 P-glycoprotein (P-gp) 기질로 알려져 있어 뇌로의 이행이 제한된다. 따라서, 본 연구에서는 *in vitro* 실험에서 P-gp를 회피하는 것으로 보이는 몇 개의 YU102 유도체들에 대해 *in vivo*에서 뇌 투과 가능성을 평가하였다. 또, 대사 안정성이 증가할 것으로 기대되는 macrocyclic 형태의 YU102 유도체들에 대해 *in vivo* & *in vitro* 안정성을 비교하였다. 이를 통해 뇌로의 이행 및 안정성이 증가된 iP 억제제들의 가능성을 평가하고자 하였다. Rat의 liver homogenate와 whole blood를 이용한 *in vitro* 안정성 실험에서 macrocyclic compounds인 DB43, DB49가 linear forms인 DB16에 비해 전반적으로 안정성이 증가하였다. 특히, 대사가 매우 빠르게 일어나는 liver homogenate에서 DB43의 경우 큰 안정성 증가를 보였다. 또, *in vivo* stability를 비교하기 위해 진행된 mouse plasma pharmacokinetic test 결과 macrocyclic compounds (DB43,

DB49)가 linear compounds (YU102, DB16)에 비해 큰 안정성과 systemic exposure을 나타냈다. DB55의 경우 DB49에 비해 안정성이 소폭 증가하였다. YU102에 비해 P-gp와 덜 interaction한 것으로 예상되는 compounds (DB16, DB43, DB49)의 뇌 투과 잠재력을 알아보기 위해 약물 주입 후 뇌에서의 target (LMP2) inhibition 정도를 측정하였다. 같은 linear form (YU102, DB16)을 비교했을 때 DB16을 주입한 mouse brain에서 약 20% 정도 target이 억제되었다. 반면에 YU102의 경우 brain target을 거의 inhibition하지 못하였다. YU102, DB16, DB43, DB49를 주입한 mouse brain에서는 vehicle group에 비해 DB43의 경우 약 8%, DB49의 경우 약 11% 감소되었다. mouse에서 이 compounds의 blood-to-plasma ratio (B/P ratio)와 plasma unbound fraction을 측정한 결과, DB43을 제외한 모든 compounds에서 1 이상의 B/P ratios, 54-77%의 unbound fraction을 나타내어 erythrocyte에 binding이 큰 것으로 생각된다. 본 연구에는 P-gp 기질성을 회피하는 성질과 구조적 변화(macrocyclization)를 통한 안정성 증가가 epoxyketone-based iP 억제제의 뇌로의 이행에 유리할 것이라는 가정 하에 진행되었으며, 그 잠재력을 생체 외 및 생체 내 실험을 통해 입증하였다. 추가 연구를 통한 근거가 더 필요하지만, 본 연구를 통해 epoxyketone-based inhibitor의 뇌 투과 가능성이 제시될 수 있다.

주요어: 면역프로테아좀 억제제, YU102, macrocyclization, 뇌 분포

학번: 2018-26406